Probing the Microscopic Corrugation of Liquid Surfaces with Gas-Liquid Collisions

Mackenzie E. King and Gilbert M. Nathanson[a]
Department of Chemistry, University of Wisconsin, 1101 University Avenue, Madison, Wisconsin 53706

Mark A. Hanning-Lee and Timothy K. Minton
Jet Propulsion Laboratory, Mail Stop 67-201, California Institute of Technology, Pasadena, California 91109
(Received 29 September 1992)

We have measured the directions and velocities of Ne, Ar, and Xe atoms scattering from perfluorinated ether and hydrocarbon liquids to probe the relationship between the microscopic roughness of liquid surfaces and gas-liquid collision dynamics. Impulsive energy transfer is governed by the angle of deflection: head-on encounters deposit more energy than grazing collisions. Many atoms scatter in the forward direction, particularly at glancing incidence. These results imply that the incoming atoms recoil locally from protruding C-H and C-F groups in hard spherelike collisions.

PACS numbers: 79.20.Rf, 34.50.Lf

Collisions between gas and liquid phase molecules mediate energy transfer, mass transport, and chemical reactions between the two phases [1]. A gas striking a liquid surface will encounter many different impact sites that are exposed by surface molecules continuously adopting new configurations as they reorient and diffuse. Gas-liquid energy exchange varies widely over these surface sites, since the instantaneous, local contour and composition of the surface govern the extent of multiple collisions and the momentum transfer and recoil direction per collision. What are the microscopic morphologies of liquid surfaces and how do they influence gas-liquid energy transfer, the first step in solvation? Are liquid surfaces so disordered that incoming atoms collectively sample most surface sites regardless of their direction of approach? Can we instead select specific impact sites and so control the surface rigidity by choosing approach angles which lead to collisions with different parts of the surface molecules? To begin answering these questions, we have measured the recoil directions and energies of Ne, Ar, and Xe striking two low vapor pressure liquids.

The liquids are pictured in Fig. 1. Squalane (99.9%, Aldrich), 2,6,10,15,19,23-hexamethyltetracosane, is a long chain hydrocarbon with a vapor pressure below 10^{-7} torr. Krytox 1625 (Du Pont), $F[CF(CF_3)CF_2O]_{27(ave)}CF_2CF_3$, is a perfluorinated polyether (PFPE) with a vapor pressure of 3×10^{-10} torr. Clean surfaces of these liquids are prepared by partially immersing a vertical wheel in a liquid reservoir at 290 K. The rotating wheel drags along a liquid film which is scraped by a sapphire plate, leaving behind a fresh 0.12 mm thick liquid layer [2]. Laser reflections from the coated wheel are sharp and deviate by less than 0.5° as the wheel rotates, indicating that the surface is macroscopically flat.

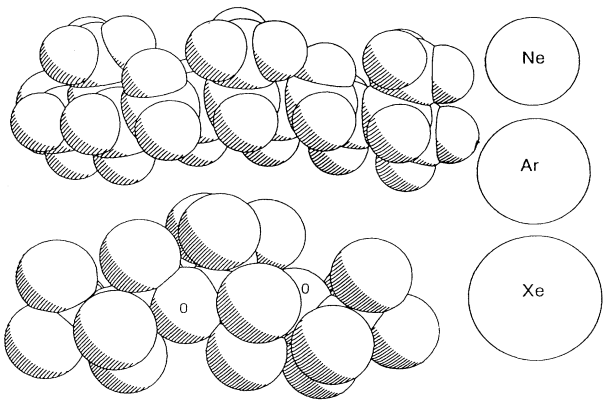

FIG. 1. Space filling models of a squalane fragment (top), $C_{14}H_{29}$, and a PFPE segment, $F[CF(CF_3)CF_2O]_2CF_2CF_3$.

An atomic beam is directed at the liquid film, which sits in a high vacuum scattering chamber, and the final translational energies E_f of atoms exiting from the liquid are determined by recording their flight times from a spinning slotted wheel to a mass spectrometer 30.3 cm away [3]. The surface and detector rotate about the same axis, so that energy transfer and scattered flux can be determined as a function of the incident and final angles θ_i and θ_f. Atomic beams are generated by expanding Ne, Ar, and Xe mixed with He or H_2 at 250 torr through a 0.11 mm aperture at 333 K. The peak incident energies $E_i \pm \sigma$ are 32 ± 4 kJ/mol for Ne, 80 ± 7 kJ/mol for Ar, and 185 ± 13 kJ/mol for Xe. For comparison, $\langle E_f \rangle \pm \sigma$ is 4.8 ± 3.4 kJ/mol for a species thermally desorbing from the 290 K liquid.

Figure 2 shows time-of-flight (TOF) spectra of Xe and Ar scattering from squalane and PFPE at $\theta_i = 45°$. Most spectra display a sharp and fast peak on top of a broader and slower component. The positions and relative sizes of the fast peaks change substantially with exit angle. Atoms in the fast channel recoil impulsively from the liquids at high velocities, transferring only a fraction of their energy to the liquid phase molecules through one or a few collisions. The slow component reflects extensive energy transfer before the atoms depart at low velocities [4]. The average energy of the slow Xe atoms, however, is $\approx 30\%$ greater than expected for thermal desorption from the 290 K liquid. These higher energies may arise

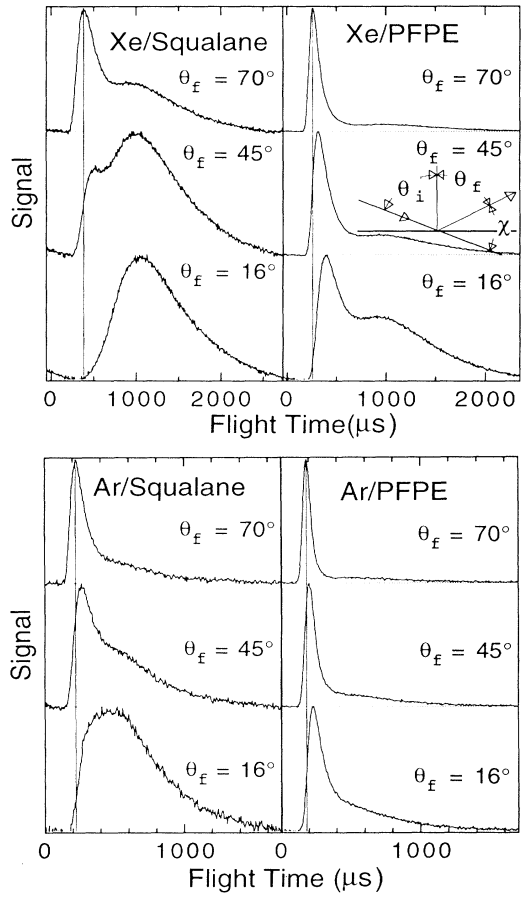

FIG. 2. TOF spectra of Xe and Ar scattering from PFPE and squalane at $\theta_i = 45°$ and $E_i = 185$ kJ/mol (Xe) and 80 kJ/mol (Ar). Each spectrum is normalized to 1; the signal is roughly twice as large from PFPE as from squalane. Elastically scattered Xe and Ar would arrive at 180 and 151 μs, respectively. The vertical lines highlight how the fast components shift with θ_f.

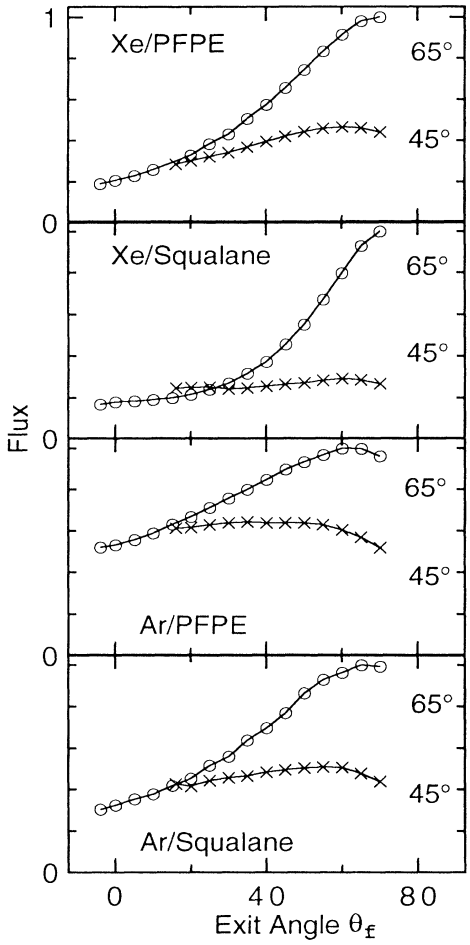

FIG. 3. Flux-weighted total angular distributions at $\theta_i = 45°$ and 65°. The maximum value in each panel is normalized to 1.

from a barrier to desorption or from an overlapping, low-energy tail of the impulsive channel due to multiple collisions.

The TOF spectra reveal that the fast peaks slow down and shrink relative to the slow components as the atoms exit at smaller θ_f, showing that energy transfer in the impulsive channel grows as θ_f decreases. These trends are also followed at $\theta_i = 25°$ and 65°. In addition, the impulsive peaks in the squalane spectra are always slower than in the PFPE spectra. The Ne spectra display similar trends, but are dominated by a fast peak with little thermal desorption. Energy transfer into the intermolecular and intramolecular modes of both liquids is extensive [1]. Squalane, however, absorbs more energy than PFPE at all measured scattering geometries, in accord with kinematic models which predict greater energy transfer to the lighter hydrocarbon than to the heavier PFPE [1,5].

The flux-weighted total angular distributions for $\theta_i = 45°$ and 65° (Figs. 3 and 4) reveal that each liquid redirects the gases widely into all measured angles, indicating that the liquids appear highly corrugated to the incoming atoms. At grazing incidence, however, the atoms scatter preferentially near the specular direction. The in-plane intensities are also greater at $\theta_i = 65°$ than at 45°. Although not shown, the angular distributions of the impulsive components follow the shapes of the total fluxes, with the exception of a more steeply rising distribution for Xe scattering from squalane at $\theta_i = 45°$. In contrast, the slow component angular distributions are cosinelike and peak at the surface normal. The slow signals are also more intense for smaller θ_i and for collisions with squalane.

Energy transfer depends sensitively on the directions in which the atoms strike the surface and rebound. The average fractional energy transfer in the impulsive channel, $\langle \Delta E \rangle / E_i$, is calculated from the inelastic component, which is obtained by subtracting a Boltzmann distribu-

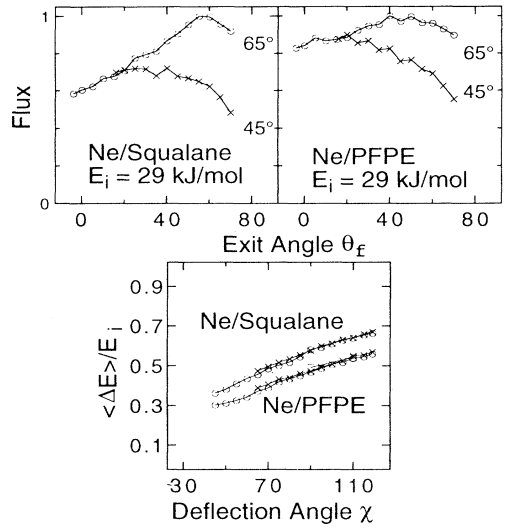

FIG. 4. Flux-weighted total angular distributions at $\theta_i = 45°$ and 65° (top) and fractional energy transfer vs $\chi = 180° - (\theta_i + \theta_f)$ (bottom) for Ne collisions.

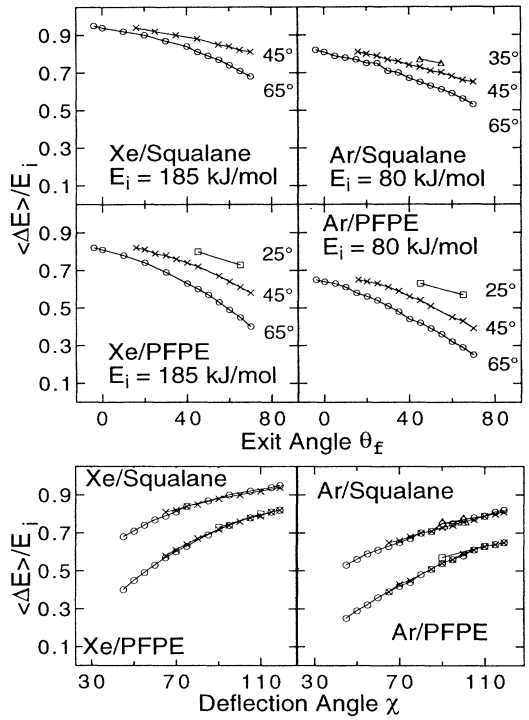

FIG. 5. Average fractional energy transfer for impulsive scattering vs θ_f and χ for different θ_i.

tion at $T_B = 290$ K from the TOF spectra. Figure 5 shows $\langle\Delta E\rangle/E_i$ for Ar and Xe as a function of θ_f. An increase in T_B from 290 to 380 K lowers $\langle\Delta E\rangle/E_i$ by less than 1% for PFPE and 6% for squalane and leaves the curves qualitatively unchanged. Figure 5 demonstrates that $\langle\Delta E\rangle/E_i$ increases when atoms either approach or exit more perpendicular to the surface. In every case, the fastest atoms recoil at grazing exit angles for grazing incident trajectories. However, many atoms scatter impulsively at angles smaller than specular and $\langle\Delta E\rangle/E_i$ increases as θ_f decreases, indicating that the colliding atoms do not conserve momentum parallel to the macroscopic surface [5,6]. Direct comparisons of TOF spectra at different θ_i reveal one further trend: The $\langle\Delta E\rangle/E_i$ values are nearly identical for scattering geometries at the same included angle $(\theta_i + \theta_f)$. This quantity is related to the angle $\chi = 180° - (\theta_i + \theta_f)$ through which the incoming atom is deflected after one or more collisions with the surface. $\langle\Delta E\rangle/E_i$ is plotted versus χ in Fig. 4 for Ne and Fig. 5 for Ar and Xe. The separate curves as functions of θ_f coalesce into a single curve as a function of χ. Within the scattering plane, *impulsive energy transfer depends only on the angle of deflection.* The figures further show that head-on or large χ collisions transfer more energy than glancing or small χ collisions.

These results are analogous to collisions with atomic solids when the incoming atom penetrates deeply enough to strike a single surface atom in single or repeated hard spherelike collisions [5,6]. Energy transfer depends on the direction and position of approach of the gas atom as it strikes a protruding surface atom. Near head-on collisions with the uphill or front side of a surface atom lead to backward or subspecular deflections and to small impact parameters, resulting in large momentum transfers along the line of centers. These large χ collisions transfer energy efficiently. Atoms at grazing incidence striking near the top or on the downhill side of the protruding atom are deflected only slightly, and these small χ collisions lead to modest energy transfers. The data in Figs. 4 and 5 follow these trends and imply that the Ne, Ar, and Xe undergo one or more hard spherelike collisions with the protruding C-H and C-F groups of the squalane and PFPE molecules shown in Fig. 1. Simulations of alkane surfaces suggest that these incoming atoms will collide in an interfacial region ≈ 10 Å thick with CH_3 end groups pointing outward or with CH_2 inner groups aligned slightly parallel to the surface [7].

We can also interpret the forward peaked angular distributions at large θ_i in terms of hard spherelike collisions. Since the incident beam samples all accessible surface sites, the local impact angle cannot be selected experimentally. The macroscopic impact angle θ_i, however, limits the minimum deflection angle and the incident atom can escape from the surface only if $\chi > 90° - \theta_i$. Large deflections at small θ_i may arise from near head-on collisions or multiple scattering events on a rough surface. These encounters lead to efficient energy transfer, enhanced thermal desorption, and the broad scattering seen in Figs. 3 and 4. At larger θ_i, smaller χ collisions occur as some atoms at grazing incidence strike protruding groups near the top or on the downhill side.

These collisions direct atoms in the forward direction. They also repress the large energy transfers and multiple collisions which would lead to thermal desorption and large signals at small θ_f. Other factors contribute to forward scattering, especially for Xe [6]. Uphill collisions leading to small θ_f at glancing incidence can be blocked by neighboring surface atoms [8]. Xe is blocked over a wider range of θ_i than Ar or Ne because it is bigger, and it may see a smaller corrugation since it can strike a larger patch of the surface. High-energy Xe and Ar may also be deflected only slightly at grazing impact angles if they knock aside a chain segment projecting out of the surface. Atoms approaching near normal incidence may instead compress chain segments or become momentarily trapped in the gaps between them.

We have begun to answer the questions posed in the beginning: even long chain hydrocarbon and fluorocarbon liquids possess surfaces structured enough to scatter high velocity atoms in preferred directions and with recoil energies which depend in systematic ways on incident and final angles. The closely packed C-H and C-F groups of squalane and PFPE scatter inert gas atoms in impulsive hard spherelike collisions, absorbing energy efficiently for collisions normal to the surface but deflecting atoms at grazing incidence more elastically. At least for high-energy encounters, these results suggest that soluble species will dissolve more readily through head-on collisions with surface molecules, while glancing blows may impede the mixing of gas and liquid and slow the approach to thermal equilibrium.

This work was carried out at the University of Wisconsin and at the Jet Propulsion Laboratory, California Institute of Technology, under a contract with the National Aeronautics and Space Administration. We thank NSF for support and R. B. Gerber for helpful discussions. M.E.K. is a National Science and Engineering Research Council Graduate Fellow (Canada); G.M.N. is a NSF Presidential Young Investigator and Camille and Henry Dreyfus Teacher-Scholar; and M.A.H.-L. is a National Research Council Resident Research Associate.

[a]Author to whom correspondence should be addressed.

[1] M. E. Saecker, S. T. Govoni, D. V. Kowalski, M. E. King, and G. M. Nathanson, Science **252**, 1421 (1991).
[2] S. A. Lednovich and J. B. Fenn, AIChE J. **23**, 454 (1977).
[3] M. J. O'Loughlin, B. P. Reid, and R. K. Sparks, J. Chem. Phys. **83**, 5647 (1985).
[4] J. E. Hurst *et al.*, Phys. Rev. Lett. **43**, 1175 (1979); J. A. Barker and D. J. Auerbach, Surf. Sci. Rep. **4**, 1 (1985).
[5] E. K. Grimmelmann, J. C. Tully, and M. J. Cardillo, J. Chem. Phys. **72**, 1039 (1980); S. Cohen, R. Naaman, and J. Sagiv, Phys. Rev. Lett. **58**, 1208 (1987).
[6] C. T. Rettner, J. A. Barker, and D. S. Bethune, Phys. Rev. Lett. **67**, 2183 (1991); A. Amirav, M. J. Cardillo, P. L. Trevor, C. Lim, and J. C. Tully, J. Chem. Phys. **87**, 1796 (1987); **87**, 1808 (1987).
[7] J. G. Harris, J. Phys. Chem. **96**, 5077 (1992).
[8] W. A. Steele, Surf. Sci. **38**, 1 (1973).